PLOS ONE

RESEARCH ARTICLE

Novel coumarin-6-sulfonamide-chalcone hybrids as glutathione transferase P1-1 inhibitors

Ahmed Sabt[1☯]*, Stefanos Kitsos[2☯], Manal S. Ebaid[3], Veronika Furlan[4], Panagiota D. Pantiora[2], Magdalini Tsolka[2], Eslam B. Elkaeed[5], Mohamed Farouk Hamissa[6], Nikolaos Angelis[7], Ourania E. Tsitsilonis[7], Anastassios C. Papageorgiou[8], Urban Bren[4,9,10], Nikolaos E. Labrou[2]*

1 Chemistry of Natural Compounds Department, Pharmaceutical and Drug Industries Research Institute, National Research Center, Dokki, Cairo, Egypt, **2** Laboratory of Enzyme Technology, Department of Biotechnology, School of Applied Biology and Biotechnology, Agricultural University of Athens, Athens, Greece, **3** Department of Chemistry, College of Science, Northern Border University, Arar, Saudi Arabia, **4** Faculty of Chemistry and Chemical Engineering, University of Maribor, Maribor, Slovenia, **5** Department of Pharmaceutical Sciences, College of Pharmacy, AlMaarefa University, Diriyah, Saudi Arabia, **6** Institute of Organic Chemistry and Biochemistry, Academy of Sciences, Prague, Czech Republic, **7** Section of Animal and Human Physiology, Department of Biology, National and Kapodistrian University of Athens (NKUA), Athens, Greece, **8** Turku Bioscience Centre, University of Turku and Åbo Akademi University, Turku, Finland, **9** Faculty of Mathematics, Natural Sciences and Information Technologies, University of Primorska, Koper, Slovenia, **10** Institute of Environmental Protection and Sensors, Maribor, Slovenia

☯ These authors contributed equally to this work.
* sabt.nrc@gmail.com (AS); Lambrou@aua.gr (NEL)

Citation: Sabt A, Kitsos S, Ebaid MS, Furlan V, Pantiora PD, Tsolka M, et al. (2024) Novel coumarin-6-sulfonamide-chalcone hybrids as glutathione transferase P1-1 inhibitors. PLoS ONE 19(8): e0306124. https://doi.org/10.1371/journal.pone.0306124

Editor: Afzal Basha Shaik, Vignan Pharmacy College, INDIA

Received: March 6, 2024

Accepted: June 10, 2024

Published: August 14, 2024

Data Availability Statement: All relevant data are within the manuscript and there is Supporting Information files.

Funding: The authors extend their appreciation to the Deanship of Scientific Research at Northern Border University, Arar, KSA for funding this research work through the project number "NBU-FFR-2024-80-01". Manal S. Ebaid (MSE) The computational part was performed by VF and UB, who are grateful to the Slovenian Research and Innovation Agency (ARIS) program and project

Abstract

Multidrug resistance (MDR) mechanisms in cancer cells are greatly influenced by glutathione transferase P1-1 (hGSTP1-1). The use of synthetic or natural compounds as hGSTP1-1 inhibitors is considered an effective approach to overcome MDR. Nine compounds consisting of coumarin-6-sulfonamide linked to chalcone derivatives were synthesized and evaluated for their ability to inhibit hGSTP1-1. Among the synthetic derivatives, compounds **5g**, **5f**, and **5a** displayed the most potent inhibitory effect, with IC_{50} values of 12.2 ± 0.5 μM, 12.7 ± 0.7 and 16.3 ± 0.6, respectively. Kinetic inhibition analysis of the most potent molecule, **5g**, showed that it behaves as a mixed-type inhibitor of the target enzyme. An *in vitro* cytotoxicity assessment of **5a**, **5f,** and **5g** against the human prostate cancer cell lines DU-145 and PC3, as well as the breast cancer cell line MCF-7, demonstrated that compound **5g** exhibited the most pronounced cytotoxic effect on all tested cell lines. Molecular docking studies were performed to predict the structural and molecular determinants of **5g**, **5f**, and **5a** binding to hGSTP1-1. In agreement with the experimental data, the results revealed that **5g** exhibited the lowest docking score among the three studied inhibitors as a consequence of shape complementarity, governed by van der Waals, hydrogen bonds and a π-π stacking interaction. These findings suggest that coumarin-chalcone hybrids offer new perspectives for the development of safe and efficient natural product-based sensitizers that can target hGSTP1-1 for anticancer purposes.

grants P2-0046, P2-0438, L2-3175, J1-4398, L2-4430, J3-4498, J7-4638, J1-4414, J3-4497, J4-4633, I0-E015, and J1-2471, as well as the Slovenian Ministry of Science and Education project grant NOO. Veronika Furlan (VF) & Bren Urban (BU)

Competing interests: The authors have declared that no competing interests exist.

1. Introduction

Glutathione transferases (GSTs) catalyze the conjugation of glutathione (GSH) to the electrophilic center of xenobiotic compounds [1–4]. GSTs are ubiquitous and multifunctional enzymes that contribute to cell detoxification, metabolism, and apoptosis as well as regulation of cell proliferation and differentiation [1, 2]. Hence, GSTs play a significant role in safeguarding against harmful substances, such as anticancer drugs, pollutants, and carcinogens, by facilitating the nucleophilic attack of reduced glutathione [3, 4]. GSTs are dimeric proteins. Each subunit of the dimer contains a functional region comprising two distinct parts: a binding site for glutathione (G-site) and a binding site for electrophilic substrates (H-site) [5].

Chemotherapy is widely used for treating different types of tumors. However, a significant problem in cancer therapy is the emergence of resistance to chemotherapeutic drugs in cancer cells [6, 7]. Multidrug resistance (MDR) is defined as the ability of cancer cells to withstand the effects of various chemotherapeutic agents [8, 9]. The mechanisms underlying drug resistance include changes in drug transport, leading to reduced entry or increased efflux of drugs from tumor cells and increased expression of GSTs, thus enhancing the conjugation of chemotherapeutic agents, especialy of the alkylating agents (e.g. cisplatin, chlorambucil, melphalan, carmustine, cyclophosphamide, thiotepa) that have been used for the treatment of a wide variety of MDR cancers including multiple myeloma, lymphoma, glioma, prostate, ovarian, bladder, lung, etc [8, 10–13]. Overexpression of GSTs has been noted in a range of cancer types, such as prostate cancer, gastric carcinoma, and acute and chronic lymphoblastic leukemia [14–16]. In particular, the isoenzyme hGSTP1-1 plays an important role in multidrug resistance by increasing the GSH-conjugation of alkylating chemotherapeutic drugs and exercising a regulatory function in the mitogen-activated protein (MAP) kinase pathway. This pathway plays important roles in cellular survival and death signals via protein-protein interactions involving c-Jun N-terminal kinase 1 (JNK1) and apoptosis signal-regulating kinase (ASK1) [2, 7, 17, 18]. Moreover, recent research has revealed that the chaperone function of hGSTP1-1 plays a crucial role in modulating the activity of diverse intracellular proteins [19].

Because of its ability to promote tumor cell resistance in two ways, hGSTP1-1 is an important target for the creation of new compounds designed to combat MDR. This can be accomplished by either suppressing the catalytic function of GSTP1-1 or interfering with its interaction with stress signalling kinases [20]. Additionally, hGSTP1-1 is a desirable target for drug development because it fulfills two crucial requirements: significant association with diseases (target validation) and potential for being targeted by drugs (target tractability) [21–25]. GST inhibitors can either sensitize drug-resistant tumors overexpressing GSTs or can be used as prodrugs activated *in vivo* by GSTs [21–23]. Over the years, numerous powerful inhibitors have been created that bind either to the G-site or the H-site of the GSTs [4, 10, 21, 23]. For example, ethacrynic acid and the glutathione analogues ezatiostat (TER199) and canfosfamide (TER 286) have been clinically studied [8]. Other examples include ethacraplatin, a bifunctional drug composed of a cisplatin molecule conjugated by two ethacrynic acid ligands [26], the benzoxadiazol derivative 6-(7-nitro-2,1,3-benzoxadiazol-4-ylthio)hexanol (NBDHEX), which triggers apoptosis in several cancer cells [27], and auranofin, an antiarthritic gold phosphine compound for which recent studies showed that hGSTP1-1 is one of its targets [28].

Owing to their varied molecular compositions and significant bioavailability, natural products are employed in the field of medicinal chemistry for the development of novel chemical structures [29]. Recently, much attention has been paid to finding natural chemopreventive substances, especially polyphenolic compounds [30]. A variety of natural products, including coumarins and chalcones, have been shown to inhibit human GSTs *in vitro* [20–34]. Additionally, coumarin derivatives exhibit a variety of biological and pharmacological properties [35]

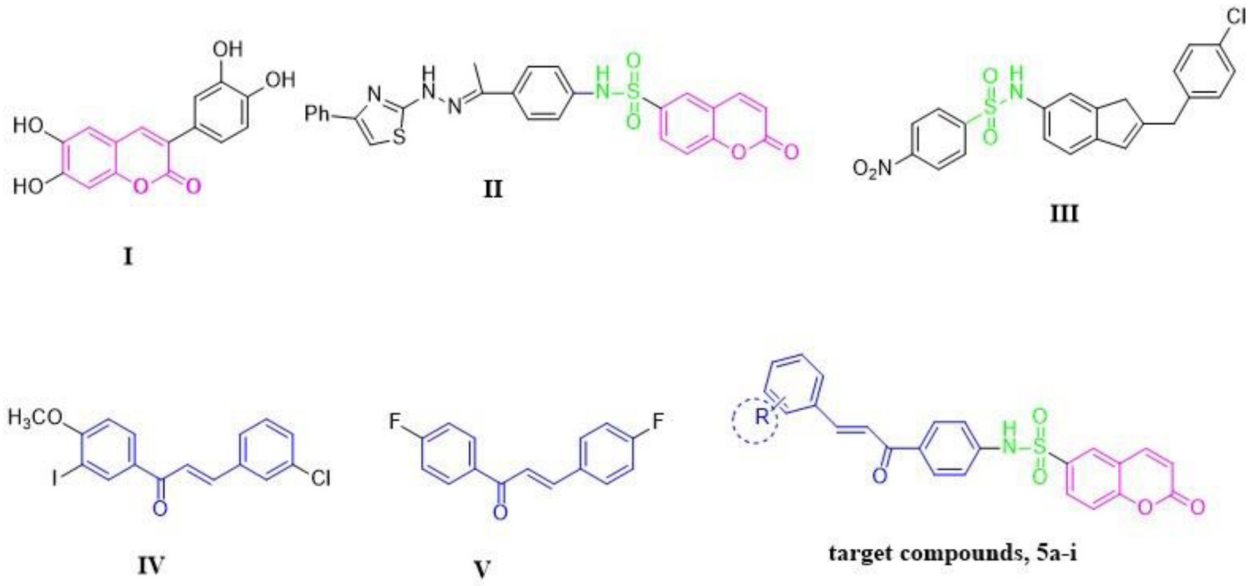

Fig 1. Structures of representative hybrids of bioactive cores I-V and the newly designed compounds 5a-i reported in the present study.

https://doi.org/10.1371/journal.pone.0306124.g001

such as anticoagulant, anti-inflammatory, antiviral, antimicrobial, antileishmanial, and anticancer [36–43]. Although there is limited research on the effects of coumarins on human GST activity, arylcoumarin **I** (Fig 1) showed significant GST inhibition [44, 45]. In 2018, Sabt *et al.* developed a new series of coumarin-6-sulfonamides with anticancer activity [40]. Among them, compound **II** (Fig 1) was the most active with IC_{50} = 3.48 ± 0.28 μM towards HepG2 cells, 1.5 times higher than doxorubicin (IC_{50} = 5.43 ± 0.24 μM). On the other hand, sulfonamide derivatives are pluripotent compounds that have shown promising biological activities, such as anti-carbonic anhydrase and anticancer properties [21, 46–49]. Additionally, a variety of compounds containing sulfonamido groups can be accommodated at the H-site of GST and act as GST inhibitors or substrates [21, 47]. For instance, compound **III** (Fig 1) showed potency similar to that of ethacrynic acid, the reference drug, as the most active hGSTP1-1 inhibitor with a value of IC_{50} = 10.2μM [50]. Both natural and synthetic chalcones are reported to have a significant potential as drugs with numerous biological activities [51, 52]. Chalcones have been found to disrupt the cell cycle and induce apoptosis. Moreover, they can inhibit tubulin polymerization and target specific kinases that are crucial for the proliferation and survival of cancer cells such as compound **IV** (Fig 1) [52]. Özaslan *et al.* developed several chalcone compounds that target GSTs, and compound **V** (Fig 1) was the most active derivative [32].

In recent years, the development of drugs in pharmaceutical and medicinal chemistry has been aided by the use of molecular hybridization. This approach involves the combination of different scaffolds to create novel analogs with enhanced biological activities [53].

The present work aimed to investigate whether coumarin-6-sulfonamide-chalcone hybrids can inhibit hGSTP1-1. For this purpose, a series of derivatives containing a coumarin core with substituted chalcone moieties was synthesized. Following their synthesis, the compounds were evaluated for their inhibitory potency against hGSTP1-1. The most effective compounds were further evaluated for their cytotoxicity against three different cancer cell lines. Additionally, molecular docking was conducted to predict the structural and molecular determinants of the interactions between the most biologically active derivatives and the target enzyme

hGSTP1-1. Overall, this study provides new insights into the design of hybrid natural products for the creation of effective and safe chemical sensitizers that specifically target hGSTP1-1.

2. Results and discussion

2.1. Synthesis and characterization of coumarin derivatives

The synthesis of the coumarin-6-sulfonamide-chalcone conjugates is shown in **Scheme 1**. The 4-aminochalcone building blocks **3a-i** were synthesized using the Claisen-Schmidt condensation of 4-aminoacetophenones and aryl aldehydes substituted with electron-withdrawing or electron-donating groups, as previously reported [54]. The reaction of coumarin-6-sulfonylchloride with 4-aminochalcone derivatives **(3a-i)** in methylene chloride in the presence of 1 mL pyridine at room temperature afforded the target coumarin-6-sulfonamide bearing chalcone derivatives **(5a-i)**. ^{1}H NMR and ^{13}C NMR spectral data were used to determine the structures of the derivatives **5a-i**. The ^{1}H NMR spectrum showed characteristic signals ranging from 7.60 to 8.08 ppm, corresponding to the hydrogens of the olefinic double bond. The observed signals manifested as doublets, occurring in pairs, with coupling constants spanning from 15.6 to 16.0 Hz, thereby suggesting a trans configuration. In the ^{13}C NMR spectrum, the most deshielded signals, exhibiting chemical shifts in the range 187–189 ppm, were attributed to the carbonyl group of the trans-enone bridge.

2.2. Enzyme inhibition analysis

By conducting enzyme activity assays, the effectiveness of the coumarin derivatives in inhibiting hGSTP1-1 was assessed at a concentration of 10 μM. As shown in Table 1, all the synthesized compounds demonstrated inhibitory activities, except for compound **5e**, which exhibited no activity. Compounds **5i, 5c, 5d, 5h,** and **5b** exhibited medium inhibition potency (45.4–71.1%), whereas compounds **5a, 5f,** and **5g** showed the highest potency (>85%) and were chosen for additional examination.

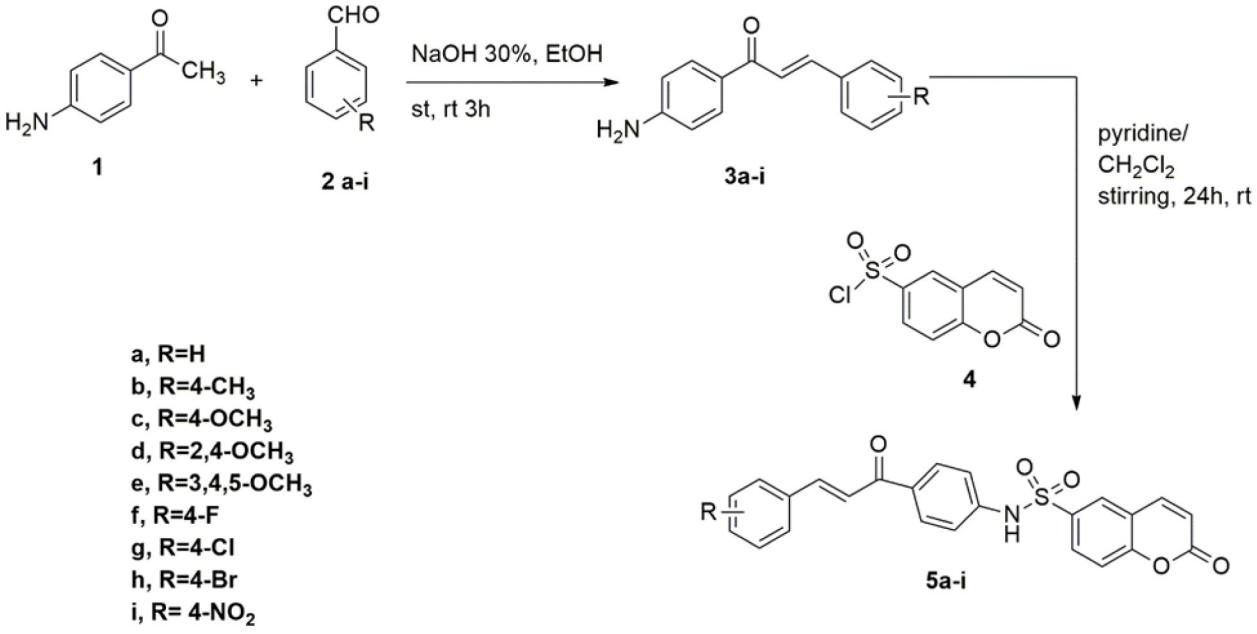

Scheme 1.

https://doi.org/10.1371/journal.pone.0306124.g002

Table 1. Assessment of hGSTP1-1 isoenzyme inhibition by coumarin derivatives. Enzyme assays were performed in triplicate, and enzyme inhibition values are expressed as the mean ± SE.

Compound	Enzyme Inhibition (%)
5a	84.6 ± 0.1
5b	62.8 ± 0.1
5c	67.0 ± 0.0
5d	59.3 ± 0.1
5e	*
5f	86.9 ± 0.0
5g	87.5 ± 0.0
5h	71.1 ± 0.1
5i	45.4 ± 0.1

* Coumarin derivative **5e** did not exhibit significant inhibition.

https://doi.org/10.1371/journal.pone.0306124.t001

Compounds that exerted the highest inhibitory activity were selected for IC_{50} determination using dose inhibition studies. A schematic representation of the results is shown in Fig 2 and a summary of the corresponding IC_{50} values is presented in **Table 2**. Coumarin derivatives **5g** and **5f** showed a significant effect on enzyme activity with similar C_{50} values of 12.2 ± 0.5 μM and 12.7 ± 0.7 μM, respectively. On the other hand, compound **5a** appeared to be a moderate inhibitor with an IC_{50} value of 16.28 ± 0.56 μM.

Several recent studies have reported the synthesis of diverse synthetic compounds that exhibit varying levels of inhibitory potency towards hGSTP1-1 or hGSTA1-1, such as benzoxadiazoles [55, 56], dihydroxybenzophenones [57], pyrroles [58], and calix [4] arenes [59]. Additionally, numerous natural products have been reported to act as potent hGSTP1-1 inhibitors [34, 60–62]. Recently, Ozalp *et al.* [63], reported a series of arylcoumarin and biscoumarin derivatives as GSTP1-1 inhibitors.

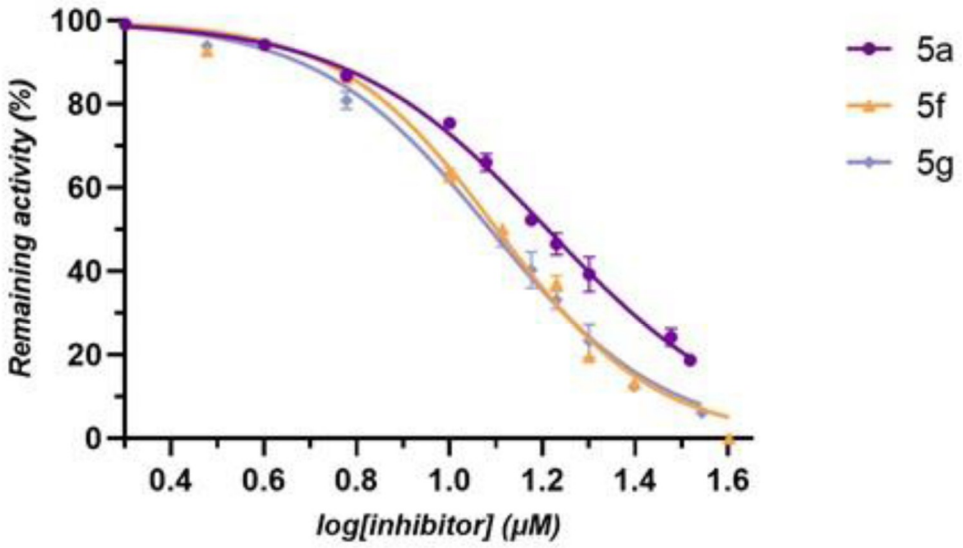

Fig 2. Concentration-response inhibition curves for the determination of IC_{50} values of the most potent inhibitors 5a, 5f, and 5g against hGSTP1-1. Data are reported as the mean ± standard error of three replicates.

https://doi.org/10.1371/journal.pone.0306124.g003

Table 2. IC_{50} values of compounds 5a, 5f, and 5g towards hGSTP1-1 obtained by concentration-response inhibition studies. All experiments were performed in triplicate, and IC_{50} values are expressed as the mean ± SE.

Compound	IC_{50} (μM)
5a	16.3 ± 0.6 μM
5f	12.7 ± 0.7 μM
5g	12.2 ± 0.5 μM

https://doi.org/10.1371/journal.pone.0306124.t002

Kinetic inhibition studies were performed using the strongest inhibitor **(5g)** to determine both the binding mode to hGSTP1-1 and the type of observed inhibition. In the presence of variable concentrations of 1-chloro-2,4-dinitrobenzene (CDNB), **5g** behaves as a non-competitive, purely mixed-type inhibitor, as indicated by the linearity of the double reciprocals (Lineweaver-Burk) graph and the derived secondary plot (Fig 3A and 3B). These results suggest that **5g** has the ability to bind to both the free hGSTP1-1, with an inhibition constant K_i of 4.69 ± 0.11 μM, and the hGSTP1-1–CDNB complex, with an inhibition constant K_i' of 19.25 ± 1.20 μM. Similarly, the same inhibitory behavior was observed when GSH was used as

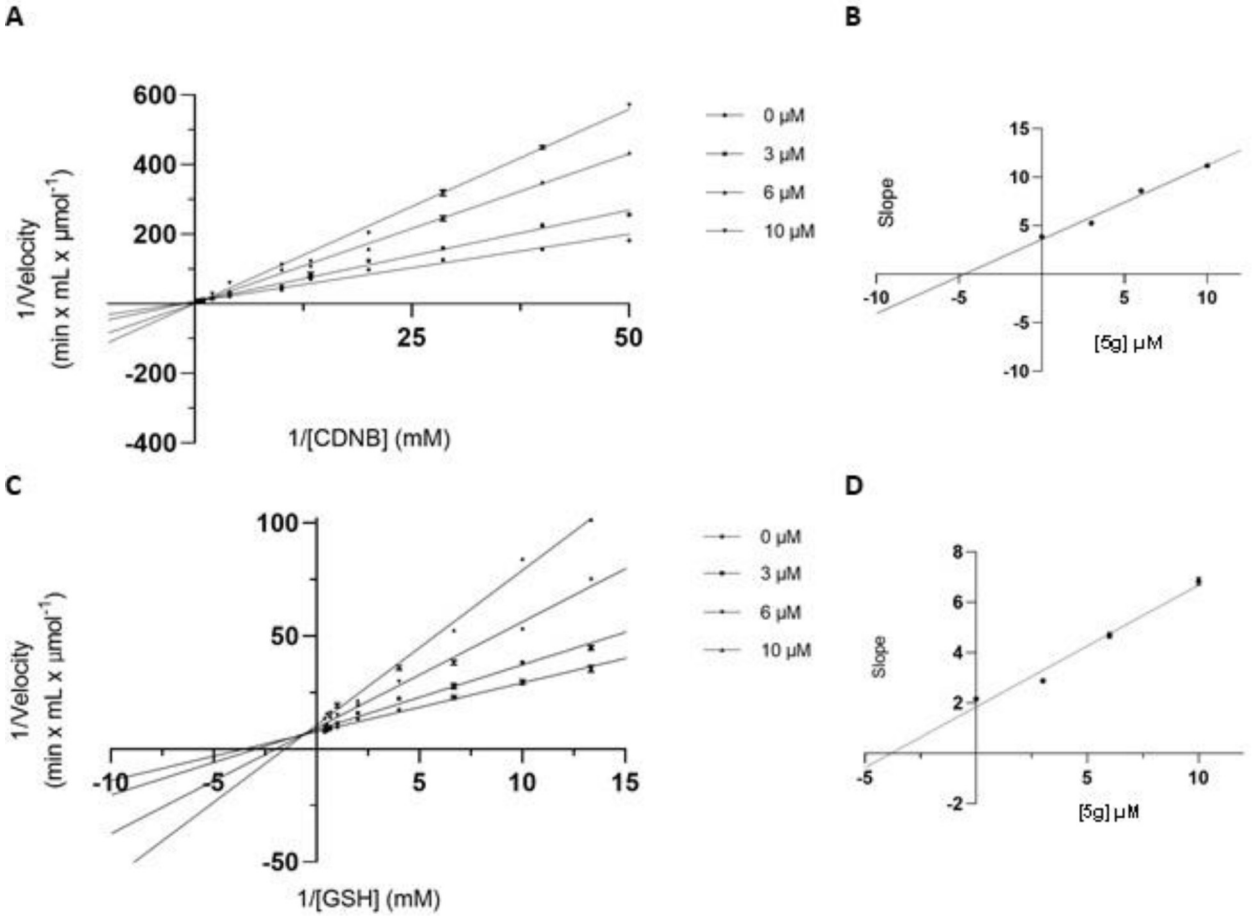

Fig 3. Kinetics inhibition studies. (A) Lineweaver–Burk plot of the inhibition of hGSTP1-1 isoenzyme using CDNB as a variable substrate (20–3,000 μM) at different constant concentrations of **5d**. (B) Secondary plot of the slopes of each Lineweaver–Burk line as a function of **5g** concentration. (C) Lineweaver–Burk plot of the inhibition of hGSTP1-1 isoenzyme using GSH as a variable substrate (75–2,500 μM) at different constant concentrations of **5g**. (D) Secondary plot of the slopes of each Lineweaver–Burk line as a function of **5g** concentration.

https://doi.org/10.1371/journal.pone.0306124.g004

the variable substrate (Fig 3C and 3D), with calculated inhibition constants K_i = 3.82 ± 0.16 μM and K_i' = 25.39 ± 0.60 μM. The large observed differences between the inhibition constants K_i and K_i' (about 4-5-times) clearly indicates that **5g** has a tendency to bind with higher affinity with the free enzyme rather with the hGSTP1-1–CDNB or hGSTP1-1–GSH complexes. Similarly, non-competitive/mixed-type inhibition has also been observed with other synthetic or natural product inhibitors of hGSTP1-1 or other evolutionarily distant GSTs [34, 55–61]. This common kinetic behavior suggests an evolutionarily conserved inhibition mechanism for all the GSTs.

2.3. Evaluation of the cytotoxic effects of coumarin derivatives on DU-145, PC3, and MCF-7 cell lines using *in vitro* methods

Cytotoxic evaluations were conducted on the most efficacious inhibitors targeting three representative cancer cell lines, namely DU-145, PC3, and MCF-7. The cytotoxicity of these inhibitors was assessed against two prostate cancer cell lines, PC3 and DU-145, and one breast cancer cell line, MCF-7. Cell viability was determined using the standard MTT protocol, and the half-maximal cytotoxic concentration (CC_{50}) values were calculated for the three most potent inhibitors **5a, 5f,** and **5g**. The results are summarized in Table 3 and the dose-dependent cytotoxicity effect of **5a, 5f,** and **5g** is illustrated in Fig 4A–4C. The results indicate an excellent correlation between the CC_{50} (Table 3) and IC_{50} values determined by enzyme kinetics analysis (Table 2). The most potent inhibitor of hGSTP1-1, **5g**, showed the greatest cytotoxicity against the three cancer cell lines. In contrast, DU-145 appeared to be the least sensitive of the three coumarin derivatives, with both PC3 and MCF-7 being the most sensitive. The cytotoxic effect of **5g** on MCF-7 cells was much greater than that of other natural substances, such as catechin and gossypol [25].

2.4. Molecular docking studies

2.4.1. Molecular docking of 5a, 5f, and 5g to hGSTP1-1. Molecular docking was performed using the CANDOCK algorithm and the RMR6 scoring function to investigate the binding mechanisms of coumarin derivatives **5a, 5f,** and **5g** in the active pocket of the target enzyme hGSTP1-1 [64]. Following an initial visual inspection, the binding patterns of **5g, 5f**, and **5a** at the active site of hGSTP1-1 were selected based on their lowest docking score values, as shown in Table 4.

As indicated in Table 4, all examined coumarin derivatives exhibited a strong affinity for binding to hGSTP1-1, with docking score values below -30 arbitrary units. The findings from the molecular docking analysis align with the experimental data obtained, suggesting that the investigated coumarin derivatives possess inhibitory properties against the target enzyme hGSTP1-1. Additionally, the molecular docking findings revealed that the coumarin derivative 5g exhibited a higher affinity for binding to hGSTP1-1 than compounds **5a** and **5f** as indicated

Table 3. Half-maximal cytotoxic concentration (CC_{50}) values for the most potent inhibitors 5a, 5f, and 5g against DU-145, PC3, and MCF-7 cell lines. All experiments were performed in triplicate, and the CC_{50} values were expressed as the mean ± SE.

Compound	CC_{50} against DU-145 (μM)	CC_{50} against PC3 (μM)	CC_{50} against MCF-7 (μM)
5a	71.4 ± 5.4	25.3 ± 2.2	46.8 ± 5.1
5f	47.3 ± 2.7	14.7 ± 0.9	24.7 ± 1.5
5g	36.6 ± 2.7	11.9 ± 2.5	17.4 ± 2.9

https://doi.org/10.1371/journal.pone.0306124.t003

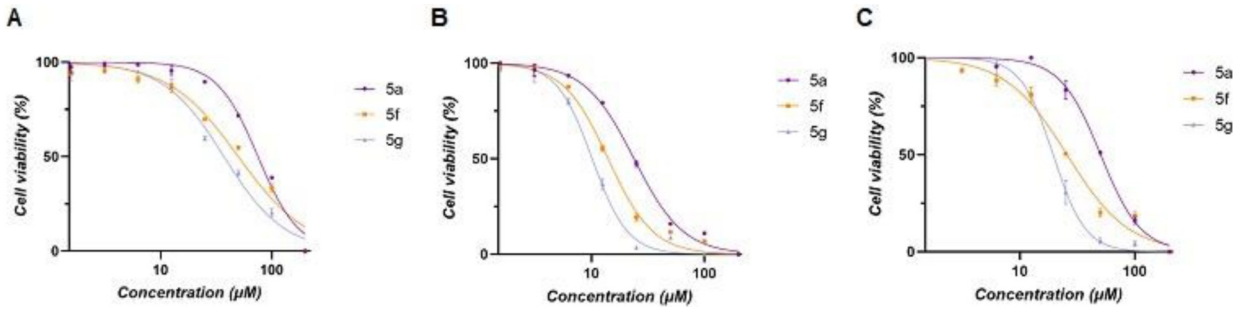

Fig 4. Dose-dependent cytotoxicity effect of the inhibitors 5a, 5f, and 5g against three human tumor cell lines. (A): DU-145; (B): PC3; (C) MCF-7. The data were analyzed using GraphPad Prism 9.3.1.

https://doi.org/10.1371/journal.pone.0306124.g005

by the lowest docking score value (-45.97 arbitrary units). As a result, **5g** was selected for further analysis.

2.4.2. Binding mode of 5a, 5f, and 5g at the active site of hGSTP1-1. The detailed interactions of **5a**, **5f**, and **5g** with hGSTP1-1 were assessed with the Protein Ligand Interaction Profiler (PLIP) [65] and the results are presented in Fig 5.

From the binding mode shown in **Fig 5**, it can be observed that coumarin derivative **5g** forms nonpolar van der Waals interactions interactions with amino acid residues Ile104, Val35, and Tyr108 at distances 3.6, 3.65, 3.7 and 3.8 Å, respectively. **5g** is additionally stabilized through a hydrogen bond with nearby residue Gln39 at a distance of 2.8 Å as well as by a π-π stacking interaction with residue Phe8 at a distance of 4.5 Å. The hydrophobic interactions from G-site are, therefore, crucial for stabilizing the **5g** inhibitor at the active site of hGSTP1-1, while hydrogen bonds play a minor role. Furthermore, the interactions of **5a** and **5f** with the binding site amino-acid residues are shown in Fig 5B and 5C, respectively. From these two figures, it can be observed that similar amino acid residues from the G-site play an important role in the binding of the coumarin derivatives to hGSTP1-1, confirming that all three derivatives (**5g**, **5f**, and **5a**) occupy the same site.

3. Conclusion

Over the past two decades, extensive studies have shed light on the role of GSTs on therapeutic response to chemotherapy. Studies have shown that GSTs play a significant role in chemotherapy through their function to deactivate anticancer drugs and/or control cell signaling pathways. In this study, we report the synthesis of novel hybrid compounds based on a coumarin-6-sulfonamide scaffold and investigate their inhibitory and cytotoxic potency against hGSTP1-1 and three cancer cell lines (DU-145, PC3, and MCF-7). The results revealed that **5g** displayed the highest inhibition and cytotoxicity potency and behaved as a mixed-type inhibitor of hGSTP1-1. It is suggested that **5g** may have a synergistic effect on the suppression (cytotoxicity) and chemosensitization (hGSTP1-1 inhibition) of cancer cells. Molecular docking indicated that hydrogen bonds, a π–π stacking interaction, and nonpolar van der Waals

Table 4. The lowest docking score values of the studied hGSTP1-1–coumarin derivative complexes.

Coumarin derivative	Docking score values (arbitrary units)
5a	-36.84
5f	-42.18
5g	-45.97

https://doi.org/10.1371/journal.pone.0306124.t004

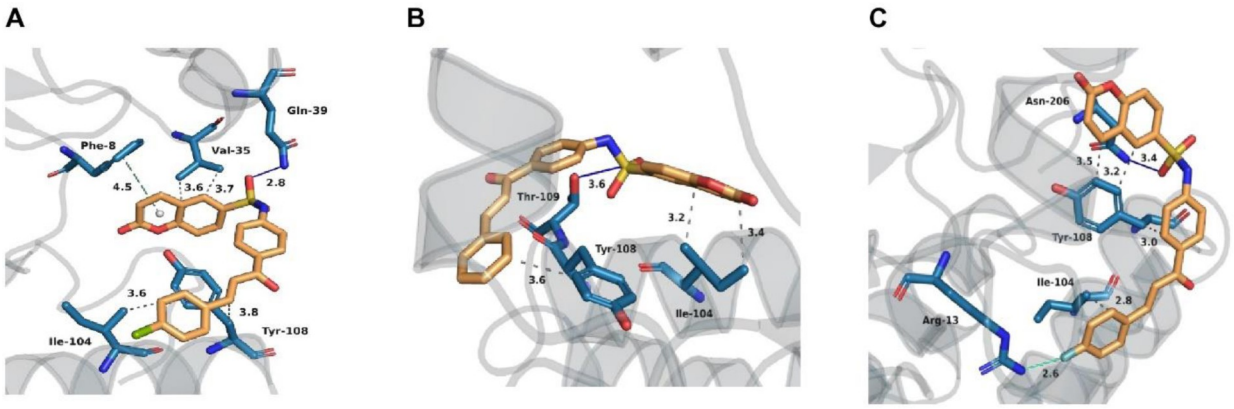

Fig 5. The predicted interaction of interaction of 5g, 5a, and 5f with hGSTP1-1. (A) Binding mode of compound **5g** at the active site of hGSTP1-1 with the lowest docking score value. (B) Binding mode of compound **5a** at the active site of hGSTP1-1 with the lowest docking score value. (C) Binding mode of compound **5f** at the active site of hGSTP1-1 with the lowest docking score value. In subfigures a), b), and c) carbon atoms of compounds **5g**, **5a**, and **5f** are depicted in orange, while carbon atoms of hGSTP1-1 amino-acid residues are presented in light blue color. The oxygen atoms are red, nitrogen atoms are dark blue, sulphur atom is yellow, chlorine atom is green, and fluorine atom is light green color. Van der Waals interactions are presented with gray dashed lines, hydrogen bonds are depicted with dark blue lines, π-π stacking interaction is presented with green dashed line, and halogen interaction with cyan line. Hydrogen atoms are omitted for reasons of clarity.

https://doi.org/10.1371/journal.pone.0306124.g006

interactions play a crucial role in the binding and inhibitory activities of **5g.** Overall, our data provide new insights into the development of natural product-based hybrid molecules that are potent inhibitors towards hGSTP1-1 and function as effective cancer chemosensitizers.

4. Experimental section

4.1. Chemistry

Melting points were determined using an Electrothermal IA 9000 apparatus and were uncorrected. Elemental analyses were performed at the Micro-Analytical Central Services Laboratory, Faculty of Science, Cairo University, Egypt. ^{1}H-NMR and ^{13}C-NMR spectra were measured using Bruker Avance II™ 400 MHz spectrometers (Bruker Biospin AG, Fällanden, Switzerland) in Prague, Czech Republic. The reactions were followed by TLC (silica gel, aluminium sheets 60 F254, Merck) using chloroform/methanol (9.5:0.5 v/v) as eluent and sprayed with iodine-potassium. Compounds **3a-i** were previously prepared [66, 67]. The characterization data of all the newly synthesized compounds are reported below.

4.1.1. General procedure for the preparation of coumarin-6-sulfonamide chalcones 5a-i. As a catalytic reaction, a mixture of coumarin-6-sulfonylchloride **(4)** (0.001 mol) and 4-amino-chalcone derivatives (0.001 mol) **3a-i** in methylene chloride and 1mL pyridine were stirred at room temperature for 24 hours. The reaction mixture was then put onto ice and acidified with diluted HCl to produce a precipitate, which was then filtered, dried, and crystalized with ethanol to get the target compounds **5a-i**.

N-(4-cinnamoylphenyl)-2-oxo-2*H*-chromene-6-sulfonamide **(5a).**

Yellow powder; yield 81%, m.p. 128–129˚C. ^{1}H NMR (400 MHz, DMSO-d_6): δ = 6.60 (d, 1H, *J* = 9.6 Hz, H3 of coumarin), 7.28 (d, 2H, *J* = 8.8 Hz, H-Ar), 7.43–7.44 (m, 3H, H-Ar), 7.57 (d, 1H, *J* = 8.8 Hz, H-Ar), 7.66 (d, 1H, *J* = 15.6 Hz, CH =), 7.83–7.86 (m, 3H, CH = and 2H-Ar), 7.96 (dd, 1H, *J* = 2.4 and 8.8 Hz, H-Ar), 8.06 (d, 2H, *J* = 8.8 Hz, H-Ar), 8.18 (d, 1H, *J* = 9.6 Hz, H4 of coumarin), 8.33 (d, 1H, *J* = 2.4 Hz, H5 of coumarin), 11.06 (s, 1H, NH), ^{13}C NMR (101 MHz, DMSO-d_6): δ = 113.43(C3 of Coumarin), 118.40, 118.45, 118.68, 119.53, 122.27, 128.31, 128.94, 129.26, 129.36, 130.00, 130.73, 131.02, 131.59, 133.24, 135.12, 135.61,

142.43, 143.79, 144.05, 156.56(C9 of Coumarin), 159.50(C2 of Coumarin), 188.18(C = O). Anal. Calcd for $C_{24}H_{17}NO_5S$ (431.46) C, 66.81; H, 3.97; N, 3.25; Found: C, 66.99; H, 4.14; N, 3.40.

2-oxo-N-(4-(3-(p-tolyl)acryloyl)phenyl)-2*H*-chromene-6-sulfonamide **(5b)**

Yellow powder; yield 77%, m.p. 202–204˚C. ^{1}H NMR (400 MHz, DMSO-d_6): δ = 2.46 (s, 3H, CH_3), 6.59 (d, 1H, *J* = 9.6 Hz, H3 of coumarin), 6.98 (d, 2H, *J* = 8.8 Hz, H-Ar), 7.26 (d, 2H, *J* = 8.8 Hz, H-Ar), 7.56 (d, 1H, *J* = 8.8 Hz, H-Ar), 7.62 (d, 1H, *J* = 15.6 Hz, CH =), 7.68 (d, 1H, *J* = 15.6 Hz, = CH), 7.78 (d, 2H, *J* = 8.8 Hz, H-Ar), 7.97 (dd, 1H, *J* = 2.4 and 8.8 Hz, H-Ar), 8.03 (d, 2H, *J* = 8.8 Hz, H-Ar), 8.17 (d, 1H, *J* = 9.6 Hz, H4 of coumarin), 8.32 (d, 1H, *J* = 2.4 Hz, H5 of coumarin), 11.01 (s, 1H, NH), ^{13}C NMR (101 MHz, DMSO-d_6): δ = 26.87(CH_3), 114.85, 118.39, 118.43, 118.57, 118.70, 119.52, 119.72, 124.67, 127.76, 128.29, 129.99, 130.57, 131.16, 133.54, 135.62, 142.20, 143.78, 144.17, 149.46, 156.86 (C9 of Coumarin), 159.50 (C2 of Coumarin), 188.18(C = O). Anal. Calcd for $C_{25}H_{19}NO_5S$ (445.10) C, 67.40; H, 4.30; N, 3.14; Found: C, 67.58; H, 4.47; N, 3.33.

N-(4-(3-(4-methoxyphenyl)acryloyl)phenyl)-2-oxo-2*H*-chromene-6-sulfonamide **(5c)**

Yellow powder; yield 49%, m.p. 238–239˚C. ^{1}H NMR (400 MHz, DMSO-d_6): δ = 3.80 (s, 3H, OCH_3), 6.59 (d, 1H, *J* = 9.6 Hz, H3 of coumarin), 6.98 (d, 2H, *J* = 8.8 Hz, H-Ar), 7.27 (d, 2H, *J* = 8.8 Hz, H-Ar), 7.57 (d, 1H, *J* = 8.8 Hz, H-Ar), 7.63 (d, 1H, *J* = 15.6 Hz, CH =), 7.69 (d, 1H, *J* = 15.6 Hz, = CH), 7.78 (d, 2H, *J* = 8.8 Hz, H-Ar), 7.98 (dd, 1H, *J* = 2.4 and 8.8 Hz, H-Ar), 8.03 (d, 2H, *J* = 8.8 Hz, H-Ar), 8.17 (d, 1H, *J* = 9.6 Hz, H4 of coumarin), 8.33 (d, 1H, *J* = 2.4 Hz, H5 of coumarin), 11.02 (s, 1H, NH), ^{13}C NMR (101 MHz, DMSO-d_6): δ = 55.83(OCH_3), 114.85, 118.38, 118.43, 118.71, 119.52, 119.71, 127.75, 128.29, 130.00, 130.57, 131.16, 133.55, 135.63, 142.21, 143.78, 144.05, 156.50 (C9 of Coumarin), 159.50 (C2 of Coumarin), 161.77 (OCH_3-C), 187.88(C = O). Anal. Calcd for $C_{25}H_{19}NO_6S$ (461.09) C, 65.07; H, 4.15; N, 3.04; Found: C, 65.24; H, 4.34; N, 3.19.

N-(4-(3-(2,4-dimethoxyphenyl)acryloyl)phenyl)-2-oxo-2*H*-chromene-6-sulfonamide **(5d)**

Yellow powder; yield 71%, m.p. 208–210˚C. ^{1}H NMR (400 MHz, DMSO-d_6): δ = 3.83 (s, 3H, OCH_3), 3.88 (s, 3H, OCH_3), 6.60–6.63 (m, 3H, H3 of coumarin and 2H-Ar), 7.26 (d, 2H, *J* = 8.8 Hz, H-Ar), 7.57 (d, 1H, *J* = 8.8 Hz, H-Ar), 7.65 (d, 1H, *J* = 15.6 Hz, CH =), 7.84 (d, 1H, *J* = 8.4 Hz, H-Ar), 7.90 (d, 1H, *J* = 15.6 Hz, = CH), 7.97–8.01 (m, 3H, H-Ar), 8.17 (d, 1H, *J* = 10.0 Hz, H4 of coumarin), 8.32 (d, 1H, *J* = 2.0 Hz, H5 of coumarin), 11.00 (s, 1H, NH), ^{13}C NMR (101 MHz, DMSO-d_6): δ = 56.00 (OCH_3), 56.28(OCH_3), 98.74, 106.79, 116.35, 118.39, 118.43, 118.76, 119.22, 119.52, 128.28, 130.00, 130.44, 130.55, 133.75, 135.64, 138.84, 142.07, 143.80, 156.50 (C9 of Coumarin), 159.51(C2 of Coumarin), 160.39 (OCH_3-C), 163.52 (OCH_3-C), 187.99(C = O). Anal. Calcd for $C_{26}H_{21}NO_7S$ (491.10) C, 63.54; H, 4.31; N, 2.85; Found: C, 63.71; H, 4.49; N, 3.00.

2-oxo-N-(4-(3-(3,4,5-trimethoxyphenyl)acryloyl)phenyl)-2*H*-chromene-6-sulfonamide **(5e)**

Yellow powder; yield 55%, m.p. 235–237˚C. ^{1}H NMR (400 MHz, DMSO-d_6): δ = 3.70 (s, 3H, OCH_3), 3.84 (s, 6H, 2OCH_3), 6.60 (d, 1H, *J* = 9.6 Hz, H3 of coumarin), 7.18 (s, 2H, 2H-Ar), 7.27 (d, 2H, *J* = 8.8 Hz, H-Ar), 7.57 (d, 1H, *J* = 8.8 Hz, H-Ar), 7.61 (d, 1H, *J* = 15.6 Hz, CH =), 7.77 (d, 1H, *J* = 15.2 Hz, = CH), 7.98 (dd, 1H, *J* = 2.4 and 8.8 Hz, H-Ar), 8.05 (d, 2H, *J* = 8.8 Hz, H-Ar), 8.17 (d, 1H, *J* = 9.6 Hz, H4 of coumarin), 8.32 (d, 1H, *J* = 2.0 Hz, H5 of coumarin), 11.04 (s, 1H, NH), ^{13}C NMR (101 MHz, DMSO-d_6): δ = 56.56 (2OCH_3), 60.59 (OCH_3), 106.91, 118.41, 118.45, 118.64, 119.53, 121.41, 128.28, 129.99, 130.67, 130.71, 133.33, 135.64, 140.13, 142.39, 143.78, 144.52, 153.53 (OCH_3-2C), 156.51(C9 of Coumarin), 159.49 (C2 of Coumarin), 187.90 (C = O). Anal. Calcd for $C_{27}H_{23}NO_8S$ (521.11) C, 62.18; H, 4.45; N, 2.69; Found: C, 62.36; H, 4.63; N, 2.85.

N-(4-(3-(4-fluorophenyl)acryloyl)phenyl)-2-oxo-2*H*-chromene-6-sulfonamide **(5f)**

Yellow powder; yield 62%, m.p. 224–226˚C. ^{1}H NMR (400 MHz, DMSO-d_6): δ = 6.60 (d, 1H, *J* = 9.6 Hz, H3 of coumarin), 7.23–7.30 (m, 4H, H-Ar), 7.57 (d, 1H, *J* = 8.8 Hz, H-Ar), 7.65 (d, 1H, *J* = 15.6 Hz, CH =), 7.79 (d, 1H, *J* = 15.6 Hz, = CH), 7.90–7.93 (m, 2H, H-Ar), 7.98 (dd, 1H, *J* = 2.4 and 8.8 Hz, H-Ar), 8.05 (d, 2H, *J* = 8.8 Hz, H-Ar), 8.17 (d, 1H, *J* = 9.6 Hz, H4 of coumarin), 8.33 (d, 1H, *J* = 2.0 Hz, H5 of coumarin), 11.05 (s, 1H, NH), ^{13}C NMR (101 MHz, DMSO-d_6): δ = 116.26, 116.48, 118.39, 118.44, 118.57, 118.66, 119.52, 122.16, 128.31, 130.00, 130.32, 130.73, 131.56, 131.65, 131.83, 133.22, 135.61, 142.44, 142.80, 143.78, 156.51(C9 of Coumarin), 159.50 (C2 of Coumarin), 162.58 (C-F), 187.92 (C = O). Anal. Calcd for $C_{24}H_{16}FNO_5S$ (449.07) C, 64.14; H, 3.59; N, 3.12; Found: C, 64.32; H, 3.78; N, 3.30.

N-(4-(3-(4-chlorophenyl)acryloyl)phenyl)-2-oxo-2*H*-chromene-6-sulfonamide **(5g).**

Pale yellow powder; yield 59%, m.p. 254–255˚C. ^{1}H NMR (400 MHz, DMSO-d_6): δ = 6.60 (d, 1H, *J* = 9.6 Hz, H3 of coumarin), 7.27 (d, 2H, *J* = 8.8 Hz, H-Ar), 7.50 (d, 2H, *J* = 8.4 Hz, H-Ar), 7.57 (d, 1H, *J* = 8.8 Hz, H-Ar), 7.64 (d, 1H, *J* = 15.6 Hz, CH =), 7.85–7.89 (m, 3H, = CH and 2H-Ar), 7.98 (dd, 1H, *J* = 2.0 and 8.8 Hz, H-Ar), 8.05 (d, 2H, *J* = 8.8 Hz, H-Ar), 8.18 (d, 1H, *J* = 9.6 Hz, H4 of coumarin), 8.33 (d, 1H, *J* = 2.0 Hz, H5 of coumarin), 11.06 (s, 1H, NH), ^{13}C NMR (101 MHz, DMSO-d_6): δ = 118.41, 118.46, 118.64, 119.53, 123.03, 128.31, 129.40, 130.00, 130.79, 130.97, 133.12, 134.12, 135.49, 135.60, 142.51, 142.56, 143.79, 156.52(C9 of Coumarin), 159.50(C2 of Coumarin), 187.91(C = O). Anal. Calcd for $C_{24}H_{16}ClNO_5S$ (465.04) C, 61.87; H, 3.46; N, 3.01; Found: C, 62.05; H, 3.61; N, 3.18.

N-(4-(3-(4-bromophenyl)acryloyl)phenyl)-2-oxo-2H-chromene-6-sulfonamide **(5h)**

Pale yellow powder; yield 38%, m.p. 233–235˚C. ^{1}H NMR (400 MHz, DMSO-d_6): δ = 6.59 (d, 1H, *J* = 9.6 Hz, H3 of coumarin), 7.26 (d, 2H, *J* = 8.8 Hz, H-Ar), 7.46–7.50 (m, 1H, H-Ar), 7.55–7.67 (m, 3H, CH = and 2H-Ar), 7.78–7.89 (m, 3H, = CH and 2H-Ar), 7.97 (dd, 1H, *J* = 2.0 and 8.4 Hz, H-Ar), 8.05 (d, 2H, *J* = 8.8 Hz, H-Ar), 8.17 (d, 1H, *J* = 9.6 Hz, H4 of coumarin), 8.32 (d, 1H, *J* = 2.0 Hz, H5 of coumarin), 11.05 (s, 1H, NH), ^{13}C NMR (101 MHz, DMSO-d_6): δ = 118.39, 118.45, 118.63, 119.52, 123.07, 124.36, 128.31, 129.38, 129.99, 130.32, 130.78, 130.95, 131.16, 132.31, 133.11, 134.11, 134.41, 135.60, 142.51, 143.78, 149.20, 156.47 (C9 of Coumarin), 159.49 (C2 of Coumarin), 187.90 (C = O). Anal. Calcd for $C_{24}H_{16}BrNO_5S$ (508.99) C, 56.48; H, 3.16; N, 2.74; Found: C, 56.66; H, 3.33; N, 2.92.

N-(4-(3-(4-nitrophenyl)acryloyl)phenyl)-2-oxo-2*H*-chromene-6-sulfonamide **(5i).**

Yellow powder; yield 52%, m.p. 274–275˚C. ^{1}H NMR (400 MHz, DMSO-d_6): δ = 6.60 (d, 1H, *J* = 9.6 Hz, H3 of coumarin), 7.28 (d, 2H, *J* = 8.8 Hz, H-Ar), 7.58(d, 1H, *J* = 8.8 Hz, H-Ar), 7.73 (d, 1H, *J* = 15.6 Hz, CH =), 7.98 (dd, 1H, *J* = 2.4 and 8.8 Hz, H-Ar), 8.02 (d, 1H, *J* = 16.0 Hz, = CH), 8.08–8.13(m, 4H, H-Ar), 8.18 (d, 1H, *J* = 9.6 Hz, H4 of coumarin), 8.26 (d, 1H, *J* = 8.8 Hz, 2H-Ar-NO_2), 8.34 (d, 1H, *J* = 2.4 Hz, H5 of coumarin), 11.10 (s, 1H, NH), ^{13}C NMR (101 MHz, DMSO-d_6): δ = 118.41, 118.47, 118.60, 119.54, 124.39, 126.35, 128.32, 130.01, 130.24, 130.97, 132.79, 135.61, 141.15, 141.69, 142.81, 143.79, 148.49, 156.57 (C9 of Coumarin), 159.50 (C2 of Coumarin), 187.82 (C = O). Anal. Calcd for $C_{24}H_{16}N_2O_7S$ (476.07) C, 60.50; H, 3.38; N, 5.88; Found: C, 60.66; H, 3.52; N, 6.01.

4.2. Enzymology

4.2.1. Materials. Reduced GSH, 1-chloro-2,4-dinitrobenzene (CDNB), ampicillin, sodium dodecyl sulfate (SDS) and the chromatographic material Sepharose CL-6B were purchased from Sigma-Aldrich, USA (Merck) and were used without further treatment. Ethanol, methanol, and dimethyl sulfoxide (DMSO) were purchased from Scharlau (Spain).

4.2.2. Expression and purification of hGSTP1-1 from recombinant *E. coli* cells. The expression and purification of the hGSTP1-1 were based on a published method [34]. The purity of the enzyme was evaluated by sodium dodecyl sulphate polyacrylamide gel

electrophoresis (SDS-PAGE). Purified enzyme fractions were pooled, diluted by dropwise addition of glycerol (to 50% v/v final concentration) and stored at -20˚C.

4.2.3. Protein determination. Protein concentration was determined according to Bradford assay using bovine serum albumin as a standard [68].

4.2.4. Enzyme assays and inhibition analysis. Determination of hGSTP1-1 activity was carried out in potassium phosphate buffer (100 mM, pH 6.5, 1 mL total volume), at 25˚C using as substrates CDNB and GSH. The reaction was monitoring at 340 nm for 120 s, as described previously [34]. For inhibition analysis, coumarin derivatives were dissolved in DMSO (100 μM) and added to the assay mixture at 10 μM final concentration. The mixture was incubated at 25˚C for 1 min, prior adding the enzyme sample. The IC_{50} values were determined from a graph of the remaining GST activity (%) against inhibitor concentration. GraphPad Prism 9.3.1 (GraphPad Prism Software, Inc.) was used for determination of IC_{50} values. Kinetic inhibition analysis was performed as previously described [34] with minor modifications. Initial velocities using CDNB as a variable substrate (typically 14–1000 μM) were determined in the presence of constant concentration of GSH (2.5 mM) in the absence and presence of the coumarin derivative **5g** (0–50 μM). Initial velocities using GSH as a variable substrate (typically 37.5–3750 μM) were determined in the presence of 1 mM CDNB in the absence and presence of the coumarin derivative 5g (0–50 μM). Enzyme assays were performed in triplicates and initial velocities were corrected for spontaneous reaction rates.

4.2.5. Cytotoxicity studies of the most potent inhibitors against PC3, DU-145 and MCF-7 cancer cell lines. The MTT colorimetric assay was used to evaluate the *in vitro* cytotoxicity of **5a, 5f** and **5g** coumarin derivatives against PC3, DU-145 and MCF-7 cancer cell lines. Cancer cells were inoculated into a 96-well plate (initially at a density of 8 x 10^3 cells/well in 100 μL of culture medium) and were cultivated for 24 h, at 37˚C in a CO_2 incubator (5%). Different concentrations of 5a, 5f and 5g derivatives (1.5 μM to 200 μM), were added to cultures and incubated for 48 h. In all experiments the final DMSO concentration did not exceed 0.2% (v/v) in culture medium. The culture medium was then replaced with 100 μL of MTT solution (1 mg/mL) and after 2 h incubation, the solution was aspirated and the produced formazan crystals were dissolved in isopropanol (100 μL). The absorbance was measured at 540 nm. Dose–cell viability graphs were created using GraphPad Prism 9.3.1 and the CC_{50} values were determined.

4.3. Computational studies

4.3.1. Molecular docking. The molecular docking protocol based on the CANDOCK algorithm [64] was carried out to generate the starting models of the three most potent coumarin derivatives **5a**, **5f**, and **5g** at the active site of glutathione transferase 1–1 (hGSTP1-1). The obtained poses were evaluated by the radial-mean-reduced scoring function at a cutoff radius of 6 Å from each atom of the ligand (RMR6). The X-ray crystal structure of hGSTP1-1 (PDB ID: 18GS, chain A) was obtained from the protein data bank. The 3D structures of three studied coumarin derivatives were prepared in Avogadro [69] and subsequently geometrically optimized with the Hartree-Fock method and 6-31G(d) basis set using Gaussian 16 program [70]. As the crystal structures of **5a**, **5f**, and **5g** in complex with hGSTP1-1 have not been experimentally determined yet, the binding modes of the studied derivatives with the lowest docking score values were selected.

Supporting information

S1 File.
(PDF)

Author Contributions

Conceptualization: Ahmed Sabt, Anastassios C. Papageorgiou, Nikolaos E. Labrou.

Data curation: Ahmed Sabt, Manal S. Ebaid, Panagiota D. Pantiora, Magdalini Tsolka, Eslam B. Elkaeed, Mohamed Farouk Hamissa, Nikolaos Angelis, Ourania E. Tsitsilonis, Urban Bren, Nikolaos E. Labrou.

Formal analysis: Ahmed Sabt, Manal S. Ebaid, Veronika Furlan, Panagiota D. Pantiora, Magdalini Tsolka, Eslam B. Elkaeed, Nikolaos Angelis, Ourania E. Tsitsilonis, Urban Bren, Nikolaos E. Labrou.

Investigation: Veronika Furlan.

Methodology: Stefanos Kitsos, Veronika Furlan, Panagiota D. Pantiora, Magdalini Tsolka, Eslam B. Elkaeed, Nikolaos Angelis, Ourania E. Tsitsilonis, Urban Bren.

Software: Stefanos Kitsos, Manal S. Ebaid, Veronika Furlan.

Validation: Ahmed Sabt, Manal S. Ebaid, Eslam B. Elkaeed, Nikolaos E. Labrou.

Visualization: Ahmed Sabt, Anastassios C. Papageorgiou.

Writing – original draft: Ahmed Sabt, Anastassios C. Papageorgiou, Urban Bren, Nikolaos E. Labrou.

Writing – review & editing: Ahmed Sabt, Anastassios C. Papageorgiou, Nikolaos E. Labrou.

References

1. Hayes JD, Flanagan JU, Jowsey IR. Glutathione transferases. Annu Rev Pharmacol Toxicol. 2005; 45: 51–88. https://doi.org/10.1146/annurev.pharmtox.45.120403.095857 PMID: 15822171
2. Mazari AM, Zhang L, Ye ZW, Zhang J, Tew KD, Townsend DM. The Multifaceted Role of Glutathione S-Transferases in Health and Disease. Biomolecules. 2023; 13: 688. https://doi.org/10.3390/biom13040688 PMID: 37189435
3. Bocedi A, Noce A, Marrone G, Noce G, Cattani G, Gambardella G, et al. Glutathione Transferase P1-1 an Enzyme Useful in Biomedicine and as Biomarker in Clinical Practice and in Environmental Pollution. Nutrients. 2019 Jul 27; 11: 1741. https://doi.org/10.3390/nu11081741 PMID: 31357662
4. Zompra A, Georgakis N, Pappa E, Thireou T, Eliopoulos E, Labrou N, et al. Glutathione analogues as substrates or inhibitors that discriminate between allozymes of the MDR-involved human glutathione transferase P1-1. Pept Sci. 2016; 106: 330–344. https://doi.org/10.1002/bip.22844 PMID: 27037874
5. Dirr H, Reinemer P, Huber R. X-ray crystal structures of cytosolic glutathione S-transferases. Implications for protein architecture, substrate recognition and catalytic function. Eur J Biochem/FEBS. 1994; 220: 645–661. https://doi.org/10.1111/j.1432-1033.1994.tb18666.x PMID: 8143720
6. Mannervik B. Versatility of Glutathione Transferase Proteins. Biomolecules. 2023 Dec 6; 13: 1749. https://doi.org/10.3390/biom13121749 PMID: 38136620
7. Tew KD. Glutathione-Associated Enzymes In Anticancer Drug Resistance. Cancer Res. 2016 Jan 1; 76: 7–9. https://doi.org/10.1158/0008-5472.CAN-15-3143 PMID: 26729789
8. Allocati N, Masulli M, Di Ilio C, Federici L. Glutathione transferases: substrates, inihibitors and pro-drugs in cancer and neurodegenerative diseases. Oncogenesis. 2018 Jan 24; 7: 8. https://doi.org/10.1038/s41389-017-0025-3 PMID: 29362397
9. Pljesa-Ercegovac M, Savic-Radojevic A, Matic M, Coric V, Djukic T, Radic et al. Glutathione transferases: Potential targets to overcome chemoresistance in solid tumors. Int J Mol Sci. 2018; 19: 3785. https://doi.org/10.3390/ijms19123785 PMID: 30487385
10. Georgakis ND, Karagiannopoulos DA, Thireou TN, Eliopoulos EE, Labrou NE, Tsoungas PG, et al. Concluding the trilogy: The interaction of 2, 20 -dihydroxy-benzophenones and their carbonyl N-analogues with human glutathione transferase M1-1 face to face with the P1-1 and A1-1 isoenzymes involved in MDR. Chem Biol Drug Des. 2017; 90: 900–908. https://doi.org/10.1111/cbdd.13011 PMID: 28440951

11. Duan C, Yu M, Xu J, Li BY, Zhao Y, Kankala RK. Overcoming Cancer Multi-drug Resistance (MDR): Reasons, mechanisms, nanotherapeutic solutions, and challenges. Biomed Pharmacother. 2023; 162: 114643. https://doi.org/10.1016/j.biopha.2023.114643 PMID: 37031496

12. Ismail A, Govindarajan S, Mannervik B. Human GST P1-1 Redesigned for Enhanced Catalytic Activity with the Anticancer Prodrug Telcyta and Improved Thermostability. Cancers (Basel). 2024 Feb 12; 16: 762. https://doi.org/10.3390/cancers16040762 PMID: 38398153

13. Cui J, Li G, Yin J, Li L, Tan Y, Wei H, et al. GSTP1 and cancer: Expression, methylation, polymorphisms and signaling (Review). Int J Oncol. 2020; 56: 867–878. https://doi.org/10.3892/ijo.2020.4979 PMID: 32319549

14. Lv N, Huang C, Huang H, Dong Z, Chen X, Lu C, et al. Overexpression of Glutathione S-Transferases in Human Diseases: Drug Targets and Therapeutic Implications. Antioxidants (Basel). 2023 Nov 6; 12: 1970. https://doi.org/10.3390/antiox12111970 PMID: 38001822

15. Allen TC, Granville LA, Cagle PT, Haque A, Zander DS, Barrios R. Expression of glutathione S-transferase π and glutathione synthase correlates with survival in early stage non–small cell carcinomas of the lung. Hum Pathol. 2007 Feb 1; 38: 220–7. https://doi.org/10.1016/j.humpath.2006.07.006 PMID: 17234469

16. Peklak-Scott C, Smitherman PK, Townsend AJ, Morrow CS. Role of glutathione S-transferase P1-1 in the cellular detoxification of cisplatin. Mol Cancer Ther. 2008 Oct; 7: 3247–55. https://doi.org/10.1158/1535-7163.MCT-08-0250 PMID: 18852128

17. Zhang J, Grek C, Ye ZW, Manevich Y, Tew KD, Townsend DM. Pleiotropic functions of glutathione S-transferase P. Adv Cancer Res. 2014; 122: 143–75. https://doi.org/10.1016/B978-0-12-420117-0.00004-9 PMID: 24974181

18. Fan C, Yuan S, Zhang Y, Nie Y, Xiang L, Luo T, et al. Peroxiredoxin-1 as a molecular chaperone that regulates glutathione S-transferase P1 activity and drives mutidrug resistance in ovarian cancer cells. Biochem Biophys Rep. 2024 Jan 14; 37: 101639. https://doi.org/10.1016/j.bbrep.2024.101639 PMID: 38288281

19. He J, Yu Y, He Y, He J, Ji G, Lu H. Chemotherapy induces breast cancer stem cell enrichment through repression of glutathione S-transferase Mu. Genes Dis. 2023 May 9; 11: 528–531.https://doi.org/10.1016/j.gendis.2023.04.005 PMID: 37692524

20. Okamura T, Antoun G, Keir ST, Friedman H, Bigner DD, Ali-Osman F. Phosphorylation of Glutathione S-Transferase P1 (GSTP1) by Epidermal Growth Factor Receptor (EGFR) Promotes Formation of the GSTP1-c-Jun N-terminal kinase (JNK) Complex and Suppresses JNK Downstream Signaling and Apoptosis in Brain Tumor Cells. J Biol Chem. 2015 Dec 25; 290: 30866–78. https://doi.org/10.1074/jbc.M115.656140 PMID: 26429914

21. Axarli I, Labrou NE, Petrou C, Rassias N, Cordopatis P, Clonis YD. Sulphonamide-based bombesin prodrug analogues for glutathione transferase, useful in targeted cancer chemotherapy. Eur J Med Chem. 2009 May; 44: 2009–16. https://doi.org/10.1016/j.ejmech.2008.10.009 PMID: 19019494

22. Sau A, Pellizzari Tregno F, Valentino F, Federici G, Caccuri AM. Glutathione transferases and development of new principles to overcome drug resistance. Arch Biochem Biophys. 2010 Aug 15; 500: 116–22. https://doi.org/10.1016/j.abb.2010.05.012 PMID: 20494652

23. Perperopoulou FD, Tsoungas PG, Thireou TN, Rinotas VE, Douni EK, Eliopoulos EE, et al. 2,2'-Dihydroxybenzophenones and their carbonyl N-analogues as inhibitor scaffolds for MDR-involved human glutathione transferase isoenzyme A1-1. Bioorg Med Chem. 2014 Aug 1; 22: 3957–70. https://doi.org/10.1016/j.bmc.2014.06.007 PMID: 25002233

24. Laborde E. Glutathione transferases as mediators of signaling pathways involved in cell proliferation and cell death. Cell Death Differ. 2010 Sep; 17: 1373–80. https://doi.org/10.1038/cdd.2010.80 PMID: 20596078

25. Guneidy RA, Zaki ER, Saleh NS, Shokeer A. Inhibition of human glutathione transferase by catechin and gossypol: comparative structural analysis by kinetic properties, molecular docking and their efficacy on the viability of human MCF-7 cells. J Biochem. 2023 Dec 20; 175: 69–83. https://doi.org/10.1093/jb/mvad070 PMID: 37787553

26. Ang WH, Pilet S, Scopelliti R, Bussy F, Juillerat-Jeanneret L, Dyson PJ. Synthesis and characterization of platinum (IV) anticancer drugs with functionalized aromatic carboxylate ligands: influence of the ligands on drug efficacies and uptake. J Med Chem. 2005 Dec 15; 48: 8060–9. https://doi.org/10.1021/jm0506468 PMID: 16335930

27. Federici L, Lo Sterzo C, Pezzola S, Di Matteo A, Scaloni F, Federici G, et al. Structural basis for the binding of the anticancer compound 6-(7-nitro-2,1,3-benzoxadiazol-4-ylthio) hexanol to human glutathione s-transferases. Cancer Res. 2009 Oct 15; 69: 8025–34. https://doi.org/10.1158/0008-5472.CAN-09-1314 PMID: 19808963

28. De Luca A, Hartinger CG, Dyson PJ, Lo Bello M, Casini A. A new target for gold(I) compounds: glutathione-S-transferase inhibition by auranofin. J Inorg Biochem. 2013; 119: 38–42. https://doi.org/10.1016/j.jinorgbio.2012.08.006 PMID: 23183361

29. Ganesan A. The impact of natural products upon modern drug discovery. Curr Opin Chem Biol. 2008; 12: 306–17. https://doi.org/10.1016/j.cbpa.2008.03.016 PMID: 18423384

30. Hayeshi R, Mutingwende I, Mavengere W, Masiyanise V, Mukanganyama S. The inhibition of human glutathione S-transferases activity by plant polyphenolic compounds ellagic acid and curcumin. Food and chemical toxicology. 2007 Feb 1; 45: 286–95. https://doi.org/10.1016/j.fct.2006.07.027 PMID: 17046132

31. Das M, Bickers DR, Mukhtar H. Plant phenols as in vitro inhibitors of glutathione S-transferase (s). Biochemical and biophysical research communications. 1984 Apr 30; 120: 427–33. https://doi.org/10.1016/0006-291x(84)91271-3 PMID: 6732766

32. Özaslan MS, Demir Y, Aslan HE, Beydemir Ş, Küfrevioğlu Öİ. Evaluation of chalcones as inhibitors of glutathione S-transferase. J Biochem Mol Toxicol. 2018 May; 32: e22047. https://doi.org/10.1002/jbt.22047 PMID: 29473699

33. Appiah-Opong R, Commandeur JN, Istyastono E, Bogaards JJ, Vermeulen NP. Inhibition of human glutathione S-transferases by curcumin and analogues. Xenobiotica. 2009 Apr 1; 39: 302–11. https://doi.org/10.1080/00498250802702316 PMID: 19350453

34. Pantiora P, Furlan V, Matiadis D, Mavroidi B, Perperopoulou F, Papageorgiou AC, et al. Monocarbonyl curcumin analogues as potent inhibitors against human glutathione transferase p1-1. Antioxidants. 2022 Dec 28; 12: 63. https://doi.org/10.3390/antiox12010063 PMID: 36670925

35. Kontogiorgis C, Detsi A, Hadjipavlou-Litina D. Coumarin-based drugs: a patent review (2008–present). Expert opinion on therapeutic patents. 2012 Apr 1; 22: 437–54. https://doi.org/10.1517/13543776.2012.678835 PMID: 22475457

36. Kumar A, Kumar P, Shravya H, Pai A. Coumarins as potential anticoagulant agents. Res J Pharm Technol. 2022; 15: 1659–63. https://doi.org/10.52711/0974-360X.2022.00277

37. Hassan NW, Sabt A, El-Attar MAZ, Ora M, Bekhit AEA, Amagase K, et al. Modulating leishmanial pteridine metabolism machinery via some new coumarin-1,2,3-triazoles: Design, synthesis and computational studies. Eur J Med Chem. 2023 May 5; 253: 115333. https://doi.org/10.1016/j.ejmech.2023.115333 PMID: 37031526

38. Al-Warhi T, Sabt A, Elkaeed EB, Eldehna WM. Recent advancements of coumarin-based anticancer agents: An up-to-date review. Bioorg Chem. 2020 Oct 1; 103: 104163. https://doi.org/10.1016/j.bioorg.2020.104163 PMID: 32890989

39. Mukanganyama S, Bezabih M, Robert M, Ngadjui BT, Kapche GF, Ngandeu F, et al. The evaluation of novel natural products as inhibitors of human glutathione transferase P1-1. J Enzyme Inhib Med Chem. 2011 Aug 1; 26: 460–7. https://doi.org/10.3109/14756366.2010.526769 PMID: 21028940

40. Sabt A, Abdelhafez OM, El-Haggar RS, Madkour HM, Eldehna WM, El-Khrisy EE, et al. Novel coumarin-6-sulfonamides as apoptotic anti-proliferative agents: synthesis, in vitro biological evaluation, and QSAR studies. J Enzyme Inhib Med Chem. 2018 Jan 1; 33: 1095–107. https://doi.org/10.1080/14756366.2018.1477137 PMID: 29944015

41. Konidala SK, Kotra V, Danduga RCSR, Kola PK. Coumarin-chalcone hybrids targeting insulin receptor: Design, synthesis, anti-diabetic activity, and molecular docking. Bioorg Chem. 2020; 104: 104207. https://doi.org/10.1016/j.bioorg.2020.104207 PMID: 32947135

42. Konidala SK, Kotra V, Danduga RCSR, Kola PK, Bhandare RR, Shaik AB. Design, multistep synthesis and in-vitro antimicrobial and antioxidant screening of coumarin clubbed chalcone hybrids through molecular hybridization approach. Arab J Chem. 2021; 14: 103154. https://doi.org/10.1016/j.arabjc.2021.103154

43. Kotra SK, Kotra V, Kola PK, Devi CBP, Anusha N, Babu BH, et al. ZnCl2 catalyzed new coumarinyl-chalcones as cytotoxic agents. Saudi J Biol Sci. 2021; 28: 386–394. https://doi.org/10.1016/j.sjbs.2020.10.020 PMID: 33424321

44. Casini A, Scozzafava A, Mastrolorenzo A, Supuran LT. Sulfonamides and sulfonylated derivatives as anticancer agents. Curr Cancer Drug Targets. 2002; 2: 55–75. https://doi.org/10.2174/1568009023334060 PMID: 12188921

45. Uehara T, Minoshima Y, Sagane K, Sugi NH, Mitsuhashi KO, Yamamoto N, et al. Selective degradation of splicing factor CAPERα by anticancer sulfonamides. Nat Chem Biol. 2017; 13: 675–680. https://doi.org/10.1038/nchembio.2363 PMID: 28437394

46. Reddy NS, Mallireddigari MR, Cosenza S, Gumireddy K, Bell SC, Reddy EP, et al. Synthesis of new coumarin 3-(N-aryl) sulfonamides and their anticancer activity. Bioorg Med Chem Lett. 2004 Aug 2; 14: 4093–7. https://doi.org/10.1016/j.bmcl.2004.05.016 PMID: 15225733

47. Ruzza P, Calderan A. Glutathione Transferase (GST)-Activated Prodrugs. Pharmaceutics. 2013 Apr 2; 5: 220–31. https://doi.org/10.3390/pharmaceutics5020220 PMID: 24300447

48. Koeplinger KA, Zhao Z, Peterson T, Leone JW, Schwende FS, Heinrikson RL, et al. Activated sulfonamides are cleaved by glutathione-S-transferases. Drug Meta Dispos. 1999; 27: 986–991. PMID: 10460796

49. Ertan-Bolelli T, Musdal Y, Bolelli K, Yilmaz S, Aksoy Y, Yildiz I, et al. Synthesis and biological evaluation of 2-substituted-5-(4-nitrophenylsulfonamido) benzoxazoles as human GST P1-1 inhibitors, and description of the binding site features. ChemMedChem. 2014 May; 9: 984–92. https://doi.org/10.1002/cmdc.201400010 PMID: 24677708

50. Musdal Y, Bolelli TE, Bolelli K, Yılmaz S, Ceyhan D, Hegazy U, et al. Inhibition of human glutathione transferase P1-1 by novel benzazole derivatives. Turk J Biochem. 2012; 37: 431–436. https://doi.org/10.5505/tjb.2012.30301

51. Elkanzi NA, Hrichi H, Alolayan RA, Derafa W, Zahou FM, Bakr RB. Synthesis of chalcones derivatives and their biological activities: a review. ACS omega. 2022 Aug 2; 7: 27769–86. https://doi.org/10.1021/acsomega.2c01779 PMID: 35990442

52. Abosalim HM, Nael MA, El-Moselhy TF. Design, synthesis and molecular docking of chalcone derivatives as potential anticancer agents. Chem Select. 2021; 6: 888–95. https://doi.org/10.1002/slct.202004088

53. Viegas-Junior C, Danuello A, da Silva Bolzani V, Barreiro EJ, Fraga CA. Molecular hybridization: a useful tool in the design of new drug prototypes. Curr Med Chem. 2007; 14: 1829–52. https://doi.org/10.2174/092986707781058805 PMID: 17627520

54. Karthik R, Vimaladevi G, Chen SM, Elangovan A, Jeyaprabha B, Prakash P. Corrosion inhibition and adsorption behavior of 4–amino acetophenone pyridine 2-aldehyde in 1 m hydrochloric acid. Int J Electrochem Sci. 2015 Jun 1; 10: 4666–81. https://doi.org/10.1016/S1452-3981(23)06654-3

55. Di Paolo V, Fulci C, Rotili D, De Luca A, Tomassi S, Serra M, et al. Characterization of water-soluble esters of nitrobenzoxadiazole-based GSTP1-1 inhibitors for cancer treatment. Biochem Pharmacol. 2020; 178: 114060. https://doi.org/10.1016/j.bcp.2020.114060 PMID: 32473836

56. Cesareo E, Parker LJ, Pedersen JZ, Nuccetelli M, Mazzetti AP, Pastore A, et al. Nitrosylation of human glutathione transferase P1-1 with dinitrosyl diglutathionyl iron complex *in vitro* and *in vivo*. J Biol Chem. 2005 Dec 23; 280: 42172–80. https://doi.org/10.1074/jbc.M507916200 PMID: 16195232

57. Pouliou FM, Thireou TN, Eliopoulos EE, Tsoungas PG, Labrou NE, Clonis YD. Isoenzyme-and Allozyme-Specific Inhibitors: 2, 2′-Dihydroxybenzophenones and Their Carbonyl N-Analogues that Discriminate between Human Glutathione Transferase A1-1 and P1-1 Allozymes. Chem Biol Drug Des. 2015; 86: 1055–1063. https://doi.org/10.1111/cbdd.12574 PMID: 25891019

58. Koutsoumpli GE, Dimaki VD, Thireou TN, Eliopoulos EE, Labrou NE, Varvounis GI, et al. Synthesis and study of 2-(pyrrolesulfonylmethyl)-N-arylimines: a new class of inhibitors for human glutathione transferase A1-1. J Med Chem. 2012 Aug 9; 55: 6802–13. https://doi.org/10.1021/jm300385f PMID: 22849615

59. Kobzar O, Shulha Y, Buldenko V, Cherenok S, Silenko O, Kalchenko V, et al. Inhibition of glutathione S-transferases by photoactive calix[4]arene α-ketophosphonic acids. Bioorg Med Chem Lett. 2022 Dec 1; 77: 129019 https://doi.org/10.1016/j.bmcl.2022.129019

60. Premetis G, Marugas P, Fanos G, Vlachakis D, Chronopoulou EG, Perperopoulou F, et al. The Interaction of the Microtubule Targeting Anticancer Drug Colchicine with Human Glutathione Transferases. Curr Pharm Des. 2020; 26: 5205–5212. https://doi.org/10.2174/1381612826666200724154711 PMID: 32713331

61. Alqarni MH, Foudah AI, Muharram MM, Labrou NE. The Interaction of the Flavonoid Fisetin with Human Glutathione Transferase A1-1. Metabolites. 2021 Mar 23; 11: 190. https://doi.org/10.3390/metabo11030190 PMID: 33806779

62. Alqarni MH, Foudah AI, Muharram MM, Alam A, Labrou NE. Myricetin as a Potential Adjuvant in Chemotherapy: Studies on the Inhibition of Human Glutathione Transferase A1-1. Biomolecules. 2022 Sep 24; 12: 1364. https://doi.org/10.3390/biom12101364 PMID: 36291574

63. Ozalp L, Orhan B, Alparslan MM, Meletli F, Çakmakçı E, Danış Ö. Arylcoumarin and novel biscoumarin derivatives as potent inhibitors of human glutathione S-transferase. J Biomol Struct Dyn. 2023; 28: 1–15. https://doi.org/10.1080/07391102.2023.2262598 PMID: 37768055

64. Fine J, Konc J, Samudrala R, Chopra G. CANDOCK: Chemical atomic network-based hierarchical flexible docking algorithm using generalized statistical potentials. J Chem Inf Model. 2020; 60: 1509–1527. https://doi.org/10.1021/acs.jcim.9b00686 PMID: 32069042

65. Salentin S, Schreiber S, Haupt VJ, Adasme MF, Schroeder M. PLIP: fully automated protein-ligand interaction profiler. Nucleic Acids Res. 2015 Jul 1; 43: 443–7. https://doi.org/10.1093/nar/gkv315 PMID: 25873628

66. Patel S, Challagundla N, Rajput RA, Mishra S. Design, synthesis, characterization and anticancer activity evaluation of deoxycholic acid-chalcone conjugates. Bioorg Chem. 2022; 127: 106036. https://doi.org/10.1016/j.bioorg.2022.106036 PMID: 35878450

67. Santos MB, Pinhanelli VC, Garcia MA, Silva G, Baek SJ, França SC, et al. Antiproliferative and pro-apoptotic activities of 2′-and 4′-aminochalcones against tumor canine cells. Eur J Med Chem. 2017 Sep 29; 138: 884–9. https://doi.org/10.1016/j.ejmech.2017.06.049 PMID: 28738308

68. Bradford MM. A rapid and sensitive method for the quantitation of microgram quantities of protein utilizing the principle of protein-dye binding. Anal Biochem. 1976 May 7; 72: 248–54. https://doi.org/10.1006/abio.1976.9999 PMID: 942051

69. Hanwell MD, Curtis DE, Lonie DC, Vandermeersch T, Zurek E, Hutchison GR. Avogadro: an advanced semantic chemical editor, visualization, and analysis platform. J Cheminform. 2012; 4: 17. https://doi.org/10.1186/1758-2946-4-17 PMID: 22889332

70. Frisch MJ, Trucks GW, Schlegel HB, Scuseria GE, Robb MA, Cheeseman JR, et al. Gaussian 16, Revision B.01, Gaussian, Inc., Wallingford CT, 2016.